

OPTICS ISSUES FOR THE 4GLS HIGH-CURRENT ERL

H. L. Owen, B. D. Muratori, P. H. Williams,
STFC Daresbury Laboratory, Warrington, WA4 4AD, UK.

Abstract

4GLS is a unique 4th-generation light source delivering synchronised pulsed photon output to a suite of user experiments. An energy-recovery linac is proposed to deliver compressed 1.3 GHz, 77 pC bunches to a set of spontaneous-output undulators and to a cavity VUV free-electron laser. The problems posed by this design and the proposed solutions are discussed in this paper.

THE 4GLS FACILITY

The 4GLS facility, proposed to be constructed at Daresbury Laboratory in the UK, will consist of three inter-related accelerator systems each driving a free-electron laser; these lasers will deliver short-pulse output in the infra-red, VUV and XUV portions of the electromagnetic spectrum with pulse lengths as short as 50 fs. In combination with spontaneous output from undulators, this multi-source, multi-user facility will enable the study of real-time molecular processes on the femtosecond timescale. A conceptual design has been produced [1,2], and the scientific motivations for the project are described elsewhere [3]. The overall lattice design has been published in an EPAC 2006 paper [4] (see below for details of changes since this paper).

OPTICS IN THE HIGH-CURRENT ERL

The most challenging part of the 4GLS project is the design and construction of an energy recovery linac that will deliver 100 mA of average beam current through five insertion device straights with small transverse emittance

and short bunch lengths. A single-pass configuration is used to accelerate bunches from a ~500 kV DC photo-injector which have been pre-accelerated to 10 MeV by two five-cavity superconducting RF modules [2]. The energy-recovery linac also accelerates 1 kHz, 1 nC bunches that drive a seeded XUV-FEL [5]: 540 MeV acceleration is required by the XUV bunches, so a multi-pass ERL configuration would confer no advantages. The final bunch parameters for all three accelerator channels are summarised in Table 1. The bunch parameters in the XUV and ERL injector channels that feed into the main linac are given in Table 2.

Since the main linac accelerates two types of bunch, we would like to keep them apart so that they do not interfere. To limit space-charge growth of the ERL bunches whilst maintaining the required 100 mA average current, we utilise every 1.3 GHz radio-frequency (RF) bucket. Our proposed solution to keep the two bunch types apart is a novel scheme whereby the XUV and ERL bunches are accelerated on opposing phases of the main linac RF: both bunches thereby receive the energy chirp they require for later compression, whilst keeping quasi-independent. This scheme avoids the mutual space charge that would arise in the main linac if the bunches were co-propagating. Also, by keeping the bunches sufficiently far apart in phase – about 40 ps in our case – the trailing wakefield from the 1 nC bunch is sufficiently small by the time the 77 pC bunch passes (see Figure 2).

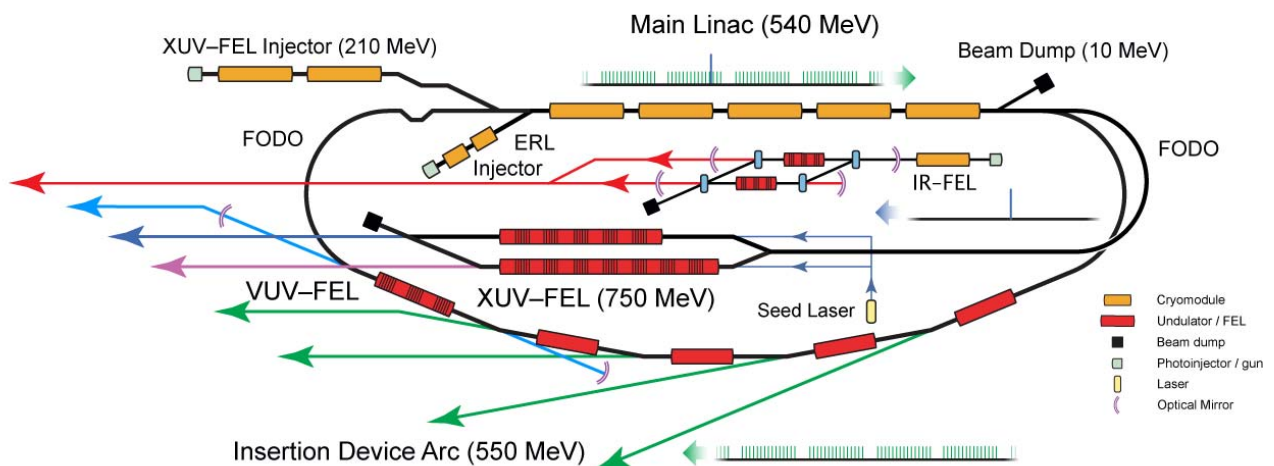


Figure 1: Schematic layout of the proposed 4GLS facility, showing the principal accelerator sections. The high-current ERL provides bunches to the outer loop of the accelerator facility, which contains five insertion devices. The last of these utilises a fully-compressed c.100 fs, 77 pC bunch to drive a regenerative-amplifier VUV-FEL.

Table 1: Output electron bunch parameters of the 4GLS facility branches.

	XUV-FEL	ERL (100 mA)	ERL (VUV-FEL)	IR-FEL
Energy	750 MeV	550 MeV		25-60 MeV
Bunch Rate	1 kHz	1.3 GHz	4.33 MHz	13 MHz
Bunch Charge	1 nC	77 pC		200 pC
Normalised Emittance	2 mm-mrad			5-10 mm-mrad
Projected Energy Spread	0.1 %			0.1% (60 MeV)
r.m.s. Bunch Length	< 270 fs	100-500 fs	100 fs	1-10 ps
Average Beam Power	1 kW	55 MW	180 kW	156 kW (60 MeV)

Table 2. Injector parameters for the 4GLS high-current and XUV branches.

	XUV-FEL	ERL (100 mA)	ERL (VUV-FEL)
Gun Output Energy	~4 MeV	~500 keV	
Injector Output Energy	210 MeV	10 MeV	
Bunch Rate	1 kHz	1.3 GHz	4.33 MHz
Bunch Charge	1 nC	77 pC	
Normalised Emittance	2 mm-mrad	2 mm-mrad	
r.m.s. Bunch Length	~3 ps	~2 ps	

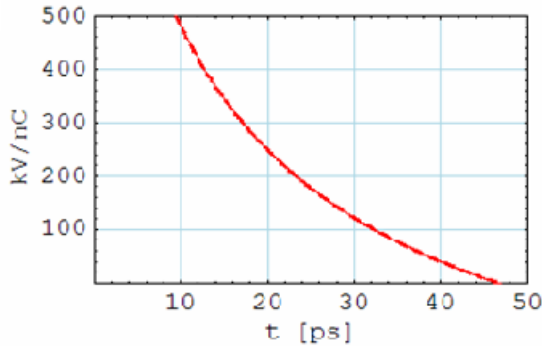


Figure 2: Trailing longitudinal cavity wakefield produced by the XUV bunches through the entire 540 MeV main linac. At 40 ps (when the 77 pC bunches pass) the energy change imparted to this bunch is small enough (around 50 keV) not to disrupt it.

Opposing-phase compression

By using opposing phase compression we gain a natural benefit in laying out the later compression. This is illustrated in Figure 3. To perform bunch compression in the energy-time plane, we imprint an energy chirp on the bunch during the main RF acceleration: we denote the sign of this compression as either A-type or B-type. A following magnetic system will shear the particles' phase space, and to compress the bunch must have a correct sign of R_{56} . We choose the *elegant* [6] sign convention whereby 4-dipole chicanes have negative R_{56} , so that an arc-like system (for instance, a double-bend achromat as shown) has therefore a positive R_{56} . An A-type chirp must be matched to an A-type compression, and conversely B

types must be matched together. Facilities such as FLASH [7] and LCLS [8] are B-type compression schemes under this notation.

Similarly, for convenience we choose that the 4GLS XUV branch is also a B-type system; this is because the final energy spread within the 1 nC XUV bunches is smaller when using a B-type scheme [9]. Conversely, the A-type scheme is simpler to achieve with the several arc cells in the ERL, and the smaller bunch charge in this branch of the accelerator means that wakefields are less of an issue. It is therefore natural to arrange an opposing-phase scheme in 4GLS with the 1 nC XUV bunches using an A-type scheme and the 77 pC ERL bunches using a B-type scheme.

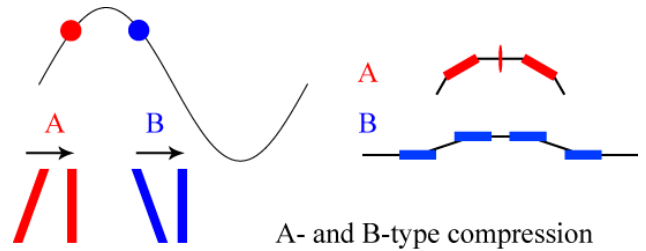


Figure 3: Illustration of the difference between A-type ('arc-like') and B-type ('bunch compressor-like') compression.

Progressive compression in the insertion devices

The undulators and VUV-FEL to be located in the five ERL insertion device straights have a requirement for both small energy spread $\sim 0.1\%$ and short bunch lengths

down to ~ 100 fs. Although the 77 pC bunch in the ERL is modest, it must still be transported through a rather long, small-aperture transport system; conversely, we predict that the effect of CSR upon the bunch transport is relatively weak [10]. Therefore, we choose to keep the bunch long in the 540 MeV linac (~ 2 ps), and then to progressively compress it through the ERL loop.

The optical scheme is shown in Figure 4: a FODO outward channel follows acceleration and performs most of the beam compression (with a total R_{56} of approximately 50cm) to reduce the bunch length from ~ 2 ps to approximately 400 fs. The remaining compression is produced by the four triple-bend achromat (TBA) cells, each of which provides a small R_{56} which is variable from 0 to 1 cm; Figure 6 shows a preliminary engineering layout of a possible TBA arc cell. Most of the user undulators will not benefit from bunch lengths as short as 100 fs, so this scheme allows us to reduce the longitudinal wakefield in these upstream straights, and thereby to minimise the undulators' vacuum apertures; initial studies [2] indicate that a Cu-coated vessel may be required in some devices.

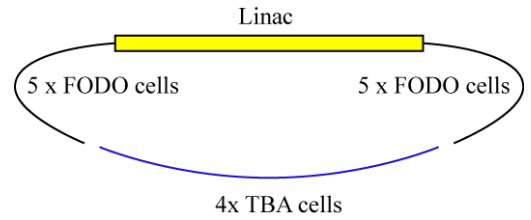


Figure 4: Optical layout of the 4GLS ERL (not including matching and beam separation).

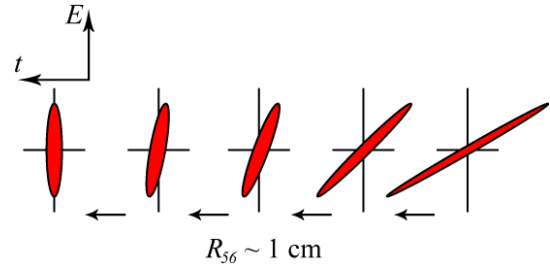


Figure 5: Principle of progressive compression proposed for the 4GLS ERL loop. The bunch is not completely compressed until the final (VUV-FEL) straight.

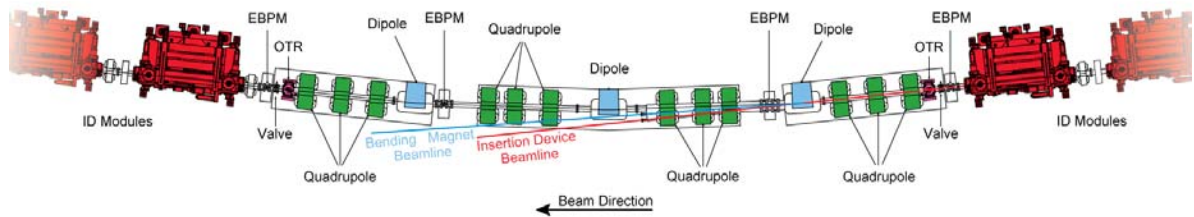


Figure 6: Preliminary ERL TBA arc cell layout;

Bunch length limit

The present optical configuration will use sextupoles in the outward FODO arc to perform linearisation of the RF curvature from the main linac. In principle, either 3rd-harmonic RF or sextupoles may perform linearisation. Figures 7 and 8 show this process schematically for 3rd-harmonic and sextupole (T_{566}) linearisation for an example system accelerating from 10 MeV to 100 MeV: in both cases we have optimised the linearisation and compression terms to give the smallest possible bunch length. It can be seen that for a long initial bunch length sextupole linearisation is not as effective as using a 3rd-harmonic cavity. Figure 8 should be compared with Figure 9, where a shorter initial bunch length is used. In the latter case the final bunch length that is achievable is much shorter, and the residual tails of Figure 8 are

essentially removed. It can thus be seen that sextupole linearisation of the main linac RF curvature is efficient for a sufficiently small initial bunch length.

A similar optimisation has been done for the more complex 4GLS ERL case, and shows that sextupole linearisation is effective if the bunch length from the high-current gun is less than 3 ps. Simulations of the high-current gun show that this bunch length is achievable [11].

ENERGY RECOVERY

The VUV-FEL is a regenerative amplifier and achieves saturation in approximately ten to fifteen passes [12]; at saturation, the final electron bunch energy spread is dominated by the lasing itself, and GENESIS 1.3 steady-state simulations [13] predict a full spread of approximately 1.2 %.

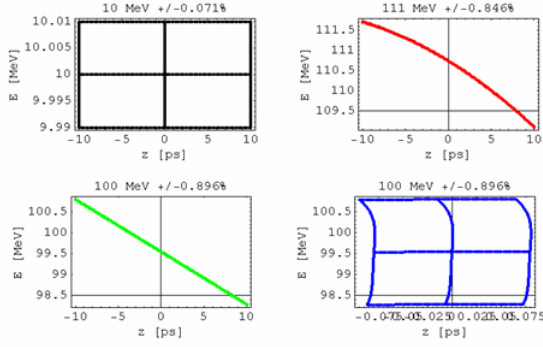


Figure 7: Sequence of acceleration and linearisation in an example system accelerating from 10 to 100 MeV. In this case, acceleration of a 10 ps-long initial bunch (black, top-left) to ~ 110 MeV (red, top-right) is followed by 3rd-harmonic linearisation (green, bottom-left). Subsequent compression (blue, bottom-right) produces a short bunch ~ 100 fs long.

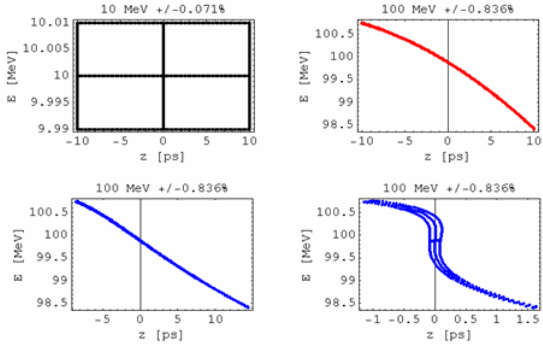


Figure 8: Sequence of acceleration and linearisation in an example system accelerating from 10 to 100 MeV. In this case, acceleration of a 10 ps-long initial bunch (black, top-left) to ~ 100 MeV (red, top-right) is followed by sextupole linearisation via T_{566} (blue, bottom-left). Subsequent compression (blue, bottom-right) cannot completely compress the bunch.

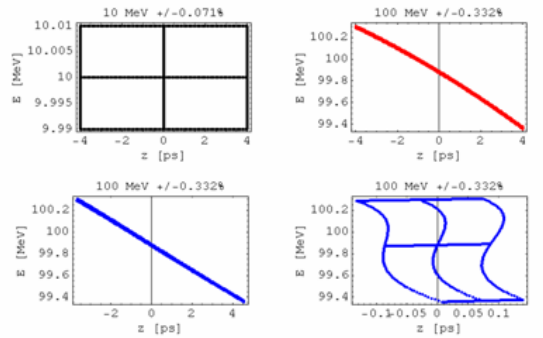


Figure 9: As Figure 8, except that the initial bunch length is 4 ps rather than 10 ps. Sextupole linearisation is effective for a short enough initial bunch length.

A simple model of FEL lasing allows us to examine the scaling of laser power with energy spread at the dump. It can be shown [14] that, for small initial electron beam energy spread, the energy spread after lasing is

$$\sigma_{FEL} \sim \rho A^2,$$

where ρ is the FEL Pierce parameter and $A \sim 1$ is the scaled field amplitude. The mean relative energy loss has the same value, so that

$$\sigma_{FEL} \sim \frac{\langle \Delta E \rangle}{E_{FEL}} \sim \rho A^2$$

In the case that the absolute energy spread is conserved in an ERL (which is only partly true – see below) it is straightforward to show that the FEL average power must be less than the beam power incident on the beam dump, since the relative energy spread at the dump must of course be less than 100%. The photon energy per pulse is just

$$E_p = n_e \langle \Delta E \rangle \ll E_r$$

where E_r is the average dump energy. For a bunch frequency f , we have simply

$$P_{FEL} = fE_p, \quad P_{dump} = n_e fE_r,$$

therefore

$$P_{FEL} \ll P_{dump}.$$

For 4GLS, since the maximum dump power is simply the beam power at 10 MeV – 1 MW, the average FEL power is limited to around 100 kW whatever the bunch frequency; power limits on the VUV-FEL mirrors will impose a much lower limit than that. However, we can express the power limit as a limit from the energy spread as

$$P_{FEL} < \sigma_r \frac{q_r f E_r}{e},$$

where σ_r is the relative energy spread at the dump. Limiting the final energy spread to 10% gives an average power limit for the 4GLS VUV-FEL of 300 W, assuming the bunch repetition rate is 4.33 MHz (see Table 1).

Although the absolute energy spread can be changed somewhat by the deceleration process, we still have a scaling of the energy spread at the dump with extracted laser pulse energy. A one-dimensional simulation of the 4GLS lasing is shown in Figure 10, where we have optimised the compression and sextupole linearisation to give the smallest possible energy spread at the dump. Although the final energy spread is smaller than the above limits suggest, as the energy spread from lasing increases so does the energy spread at the dump.

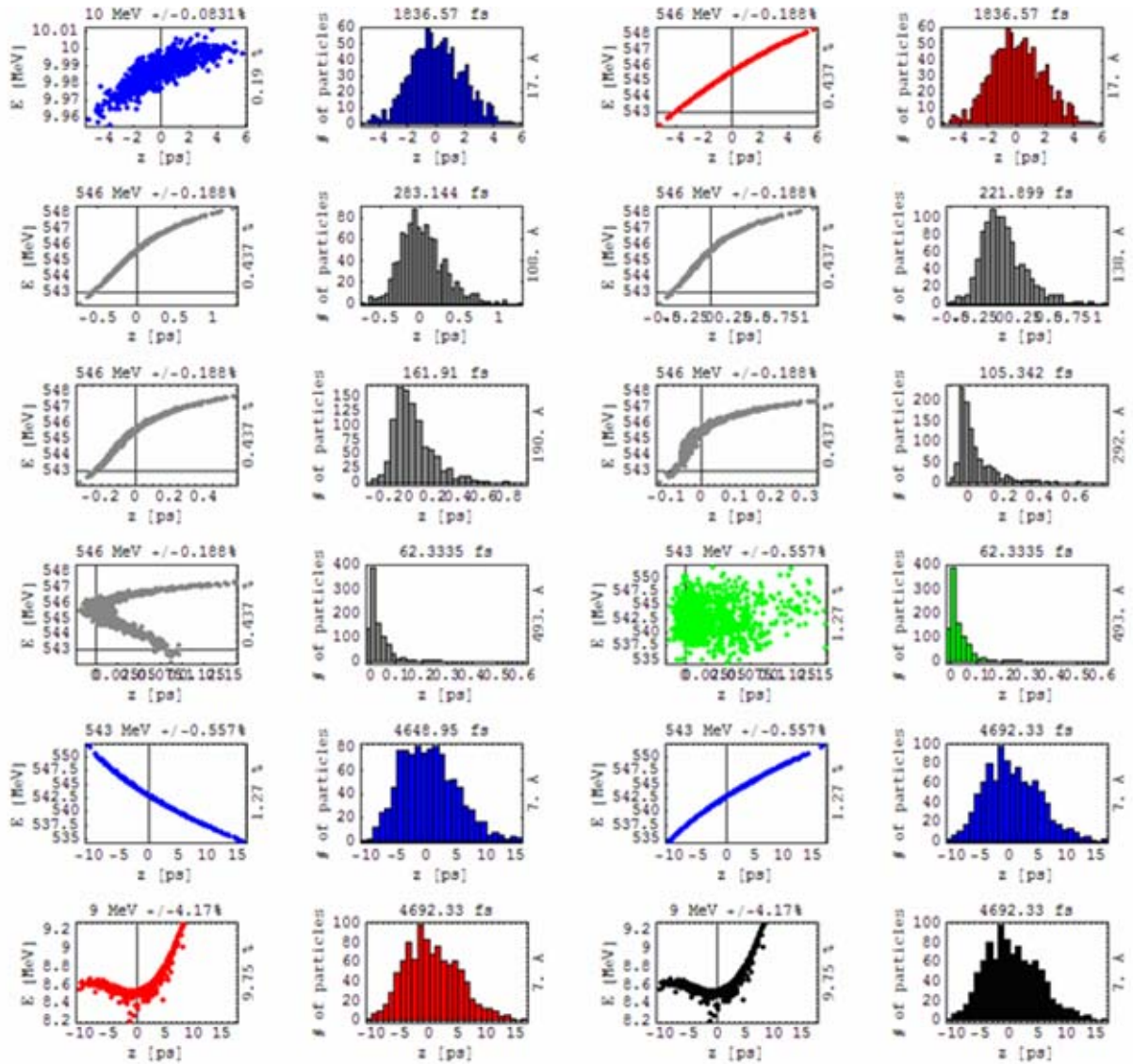


Figure 10: 1D-model of the 4GLS ERL compression, including a simple lasing model but neglecting collective and wakefield effects. The 77 pC ERL bunches are pre-accelerated and chirped prior to entering the main linac (blue, top-left). After acceleration to 550 MeV (red, top-right), they are then compressed in the outward FODO arc (grey, 2nd row) and then progressively compressed to each of the insertion device straights (following grey sections). Lasing (green, right, 4th row) increases the energy spread, and the bunch is then transported back to the main linac via the return FODO arc and final compressor section (blue, 5th row). Deceleration (red, bottom-left) and extraction to dump (black, bottom-right) show that the energy spread in the extraction region may be well-controlled.

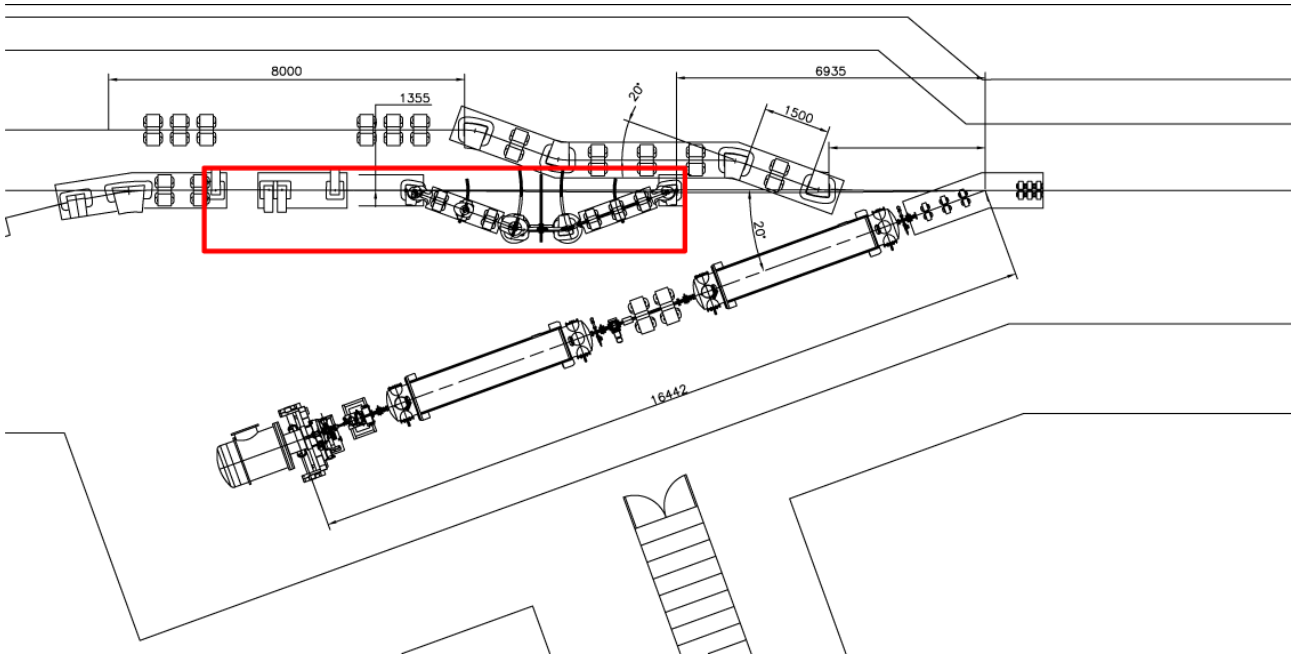


Figure 11: Outlined is placement of path correction / decompression system just prior to re-entry into the main linac.

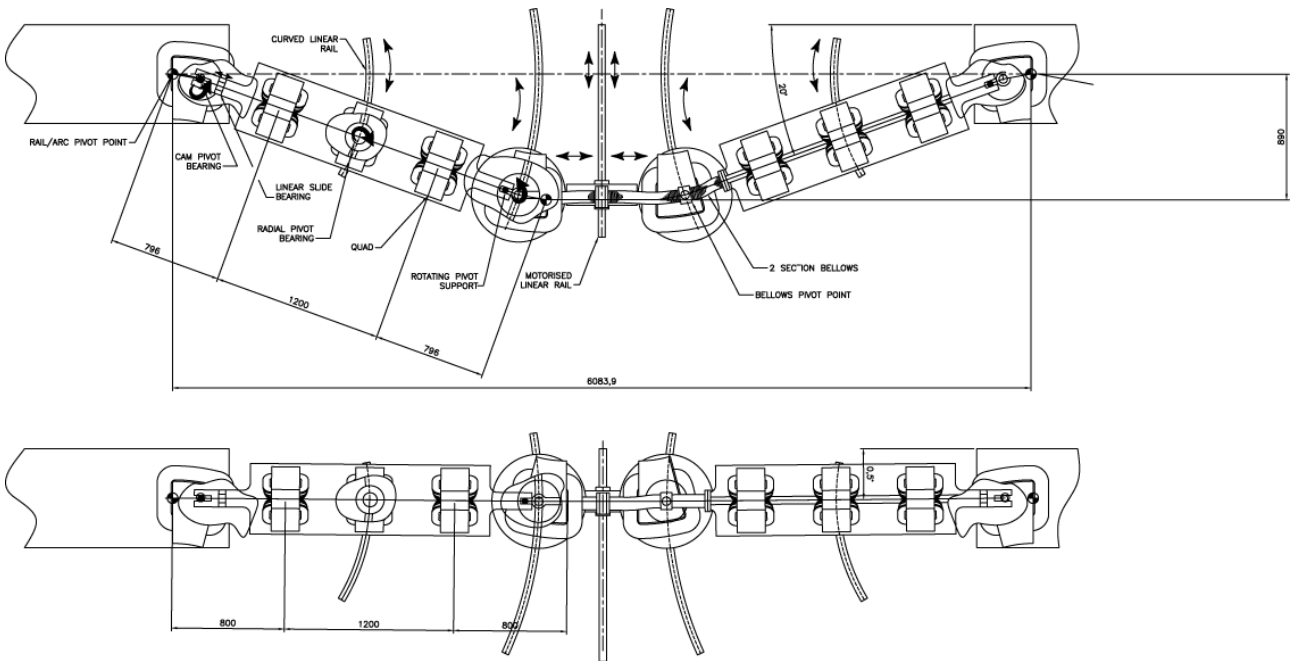


Figure 12: The moving dogleg in its maximal (above) and minimal (below) displacement configurations. This section is ~ 6 m in length and the horizontal displacement can be up to 900 mm.

PATH-LENGTH CORRECTION

In order to perform energy recovery, the bunches must return to the main linac π out of RF phase with respect to the accelerating bunches. Therefore we must be able to introduce extra path length without affecting other beam parameters through the machine. To allow flexibility in tuning and operation, and to allow the possibility of a second accelerating pass in a future upgrade, we would like to have a full wavelength (23 cm) of adjustment. A modular system decoupled from the rest of the accelerator is both more compact and will be simpler to operate.

We propose a novel system to introduce a continuously-variable path-length difference without introducing any variation of longitudinal dispersion. Our approach (Figure 11) combines a magnetic chicane (large positive R_{56} in our convention) and two physically moving, non-dispersive doglegs (small negative R_{56}). The moving doglegs are coupled by a set of bellows that expand to introduce most of the required extra path length (Figure 12). The small R_{56} induced by the changed position of the dogleg is cancelled by a small magnetic adjustment in the chicane; this ensures R_{56} remains constant as required. The entire system is located just prior to re-entry of the beam into the main linac. Including the decompression chicane, the entire system is only around 10 m long; the moving part 6 m. This should be compared to a total moving length of around 40 m if this task was performed mechanically in one of the main ERL arcs.

In principle, the system can perform the specific task of path length correction while leaving all other parameters in the accelerator unchanged. We relax this somewhat to use this section to compensate for R_{56} generated in the insertion device arc and VUV-FEL, thus ensuring correct bunch decompression for re-entry into the main linac in such a way that the energy spread at the dump is minimised.

REFERENCES

- [1] J. A. Clarke, E. A. Seddon, "The Conceptual Design of 4GLS at Daresbury Laboratory", EPAC'06, Edinburgh, <http://www.jacow.org>.
- [2] "4GLS Conceptual Design report", CCLRC Daresbury Laboratory (2006), available at www.4gls.ac.uk.
- [3] "4GLS Science Case", www.4gls.ac.uk.
- [4] M. A. Bowler, B. D. Muratori, H. L. Owen, S. L. Smith, S. V. Miginsky, "Lattice Design for the Fourth Generation Light Source at Daresbury Laboratory", EPAC '06, <http://www.jacow.org>.
- [5] B.W.J.McNeil, J.A.Clarke, D.Dunning, G.J.Hirst, N.R.Thompson, B.Sheehy & P.Williams, *New J. Physics* 9, 82 (2007).
- [6] M. Borland, OAG Software Doc. <http://www.aps.anl.gov/asd/oag/oagSoftware.html>.
- [7] J. Rossbach, *Nucl. Inst. Meth.* A375, 269 (1996).
- [8] "LCLS Design Report", SLAC-R-593/UC-414 (2002), <http://www-ssrl.slac.stanford.edu/lcls/cdr/>.
- [9] A. Novokhatski, M. Timm and T. Weiland, "Single Bunch Energy Spread in the TESLA Cryomodule", TESLA Report 99-16, DESY, Hamburg (1999).
- [10] M. A. Bowler, H. L. Owen, "A Study of CSR-Induced Microbunching Using Numerical Simulations", EPAC '04, <http://www.jacow.org>.
- [11] B. Militsyn and J. McKenzie, unpublished work.
- [12] N. R. Thompson, D. J. Dunning, B. W. J. McNeil, J. G. Karssenberg, P. J. M. van der Slot and K.-J. Boller, "A 3D Model of the 4GLS VUV-FEL Conceptual Design Including Improved Modelling of the Optical Cavity", FEL 2006, Berlin (2006), <http://www.jacow.org/>.
- [13] N. Thompson, "4GLS VUV-FEL: A Study of the FEL-Induced Beam Energy Spread", 4GLS Report fgls-fel-rpt-0004.
- [14] R. Bonfacio et al., *Rivista del Nuovo Cimento* 13(9), pp 1-69 (1990).